LETTERS | FOCUS
PUBLISHED ONLINE: 31 AUGUST 2014 | DOI: 10.1038/NMAT4072
nature materials

Entropy-driven formation of large icosahedral colloidal clusters by spherical confinement

Bart de Nijs[1†], Simone Dussi[1†], Frank Smallenburg[1], Johannes D. Meeldijk[2], Dirk J. Groenendijk[1], Laura Filion[1], Arnout Imhof[1], Alfons van Blaaderen[1*] and Marjolein Dijkstra[1*]

Icosahedral symmetry, which is not compatible with truly long-range order, can be found in many systems, such as liquids, glasses, atomic clusters, quasicrystals and virus-capsids[1–12]. To obtain arrangements with a high degree of icosahedral order from tens of particles or more, interparticle attractive interactions are considered to be essential[1,3,6–12]. Here, we report that entropy and spherical confinement suffice for the formation of icosahedral clusters consisting of up to 100,000 particles. Specifically, by using real-space measurements on nanometre- and micrometre-sized colloids, as well as computer simulations, we show that tens of thousands of hard spheres compressed under spherical confinement spontaneously crystallize into icosahedral clusters that are entropically favoured over the bulk face-centred cubic crystal structure[13,14]. Our findings provide insights into the interplay between confinement and crystallization and into how these are connected to the formation of icosahedral structures.

More than half a century has passed since Sir Charles Frank first proposed that the most favourable local structures in simple liquids have short-ranged icosahedral symmetry[12]. Such ordering occurs when 12 particles are arranged around a central particle at the vertices of an icosahedron. This icosahedron tends to minimize the short-ranged (Lennard-Jones-like) attractive interactions typically present in atomic systems, and has been shown to be entropically favourable as well[15,16]. However, its five-fold symmetry is incommensurate with long-range positional order, thereby acting as an obstacle to the formation of crystals on a larger scale. So, even though a typical liquid often contains many local icosahedral centres[1–3,12], they rarely grow out into a crystal[4]. In the case of hard spheres, which do not attract and instead interact solely by excluded volume, (distorted) icosahedral order has been observed in the fluid phase[4], in glasses[5] and in growing crystal nuclei during crystallization[17]. The thermodynamically stable crystalline phase for hard spheres is the face-centred cubic (FCC) crystal, which maximizes the entropy at high densities[13,14]. This arrangement of spheres has the densest possible packing ($\Phi = 0.74$) at infinite pressure, and does not exhibit any five-fold symmetry[13,14]. The incompatibility of the locally favourable icosahedral symmetry with long-range three-dimensional (3D) order raises immediately the question over what length scales icosahedral order can be extended.

A dense non-crystalline packing of spheres featuring global icosahedral order was theoretically proposed by Mackay in 1962[6]. The Mackay structure (which will be described in more detail below) has been observed and studied theoretically for atomic and molecular clusters[9,10,18,19] and clusters of nanoparticles[11,20–22]. In these cases, the formation of icosahedral structures is mainly attributed to energetic interactions[7,8,11] in conjunction with kinetic effects[20], hierarchical self-assembly[18], or intricate growth mechanisms[21,22]. Furthermore, Mackay clusters of Lennard-Jones particles have been shown to correspond to minima in the free-energy landscape[23]. In contrast, in hard-sphere systems attractions are not present and finite-size clusters can be obtained by means of confinement. It is known from theory, simulations and experiments that confinement can change the equilibrium crystal structure of colloidal spheres markedly from that in the bulk, but usually only on small length scales[24,25]. Here we show by experiments and simulations that spherical confinement gives rise to purely entropy-driven icosahedral symmetry in the equilibrium phase of even very large numbers of hard spheres.

To experimentally study the behaviour of colloidal spheres in spherical confinement, we synthesized cobalt iron oxide nanoparticles[26] with a core diameter of 6.0 ± 0.29 nm (9 nm effective diameter due to interdigitating oleic acid ligands, and an effective polydispersity of 3.2%; see Supplementary Fig. 1) dispersed in a suitable (apolar) solvent. This dispersion was emulsified into an oil-in-water emulsion. Subsequently, we evaporated the solvent in the suspended emulsion droplets, causing the packing fraction of the nanoparticles in the droplets to increase slowly, which eventually caused crystallization of the nanoparticles. The same process was used for fluorescently labelled micrometre-sized core–shell silica colloids[27], simply called 'colloids' in the remainder of the paper, with a diameter of $1.32 \pm 0.039\,\mu$m (and a polydispersity of 1.7%; see Supplementary Fig. 2), as well as for core–shell semiconductor nanoparticles with a core diameter of 12.4 ± 1.0 nm (14.5 nm effective diameter, and an effective polydispersity of 6.9%; results shown in Supplementary Figs 1 and 4). The colloids were dispersed in a water-in-oil emulsion instead of an oil-in-water emulsion. In all cases, the evaporation times were much longer than the diffusional equilibration time of the colloidal systems. The resulting clusters obtained via this self-assembly process, which we denote as 'supraparticles', were almost entirely crystalline. To illustrate this, in Fig. 1 we show secondary electron scanning transmission electron microscopy (SE-STEM) images of typical supraparticles of cobalt iron oxide nanoparticles. Remarkably, we observed three different types of crystalline packing, depending on the cluster size. Figure 1a shows a 105 nm diameter supraparticle that exhibits icosahedral symmetry, closely resembling the packing proposed by Mackay[6] and analogous to the clusters of gold nanoparticles formed by a similar process in ref. 11. As we will show below, it consists of twenty deformed FCC ordered tetrahedral domains that share a

[1]Soft Condensed Matter, Debye Institute for Nanomaterials Science, Utrecht University, Princetonplein 5, 3584 CC Utrecht, The Netherlands. [2]Electron Microscopy Group, Utrecht University, Padualaan 8, 3584 CH Utrecht, The Netherlands. †These authors contributed equally to this work.
*e-mail: A.vanBlaaderen@uu.nl; M.Dijkstra1@uu.nl

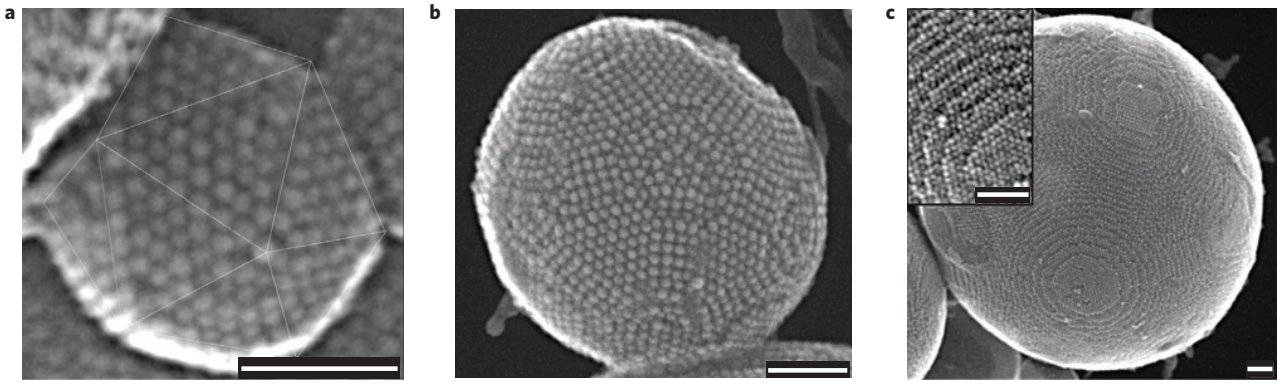

Figure 1 | Secondary electron scanning transmission electron microscopy (SE-STEM) images of typical supraparticles containing cobalt iron oxide nanoparticles. **a**, Supraparticle with a diameter of 105 nm with Mackay icosahedral symmetry, as indicated by the thin lines. **b**, 216 nm supraparticle with anti-Mackay rhombicosidodecahedral structure. **c**, 734 nm supraparticle consisting of a single face-centred cubic (FCC) crystal domain. Inset: a magnified view of the step edges of the FCC supraparticle. All scale bars are 50 nm.

particle in the centre, such that the (111) adjacent tetrahedral faces form twinning planes. The resulting supraparticle is a multiply-twinned crystal with five-fold symmetry, and has the shape of an icosahedron with 20 triangular (111) facets at the surface. For larger supraparticles, however, we find a different surface, shown in Fig. 1b, where a 216 nm supraparticle is depicted. The surface particles are arranged in a rhombicosidodecahedral geometry consisting of twelve pentagonal faces, twenty triangular faces and thirty rectangular faces. This surface-reconstructed icosahedral structure belongs to the class of the anti-Mackay icosahedra, as found for instance in clusters of argon[28] and lead[9] atoms, as well as in clusters of gold nanoparticles[11]. More precisely, these structures have a Mackay icosahedral core but a different surface termination, as the triangular facets meet yet another set of twinning planes near the surface[7]. Finally, for sufficiently large cluster sizes, the supraparticles consist of a single FCC domain of nanoparticles, as expected for systems approaching the bulk limit. Figure 1c shows an example of such a non-icosahedral FCC supraparticle with a diameter of 734 nm. In this case, the surface presents the typical step edges of an FCC crystal confined to a sphere. A further image of an FCC cluster is shown in Supplementary Fig. 3.

To confirm that the internal structure of our clusters corresponds to (anti-)Mackay icosahedra, we obtained the 3D-coordinates of the individual particles in several clusters. In particular, we extracted the positions of the nanoparticles from electron tomography images[29] (see Supplementary Movies 1 and 2), and the colloids from confocal microscopy images[30], using particle tracking software (see Supplementary Methods and Supplementary Figs 6 and 7 for more details). Figure 2 shows the structure of typical clusters, exhibiting icosahedral symmetry formed from both nanoparticles and colloids, with different colours indicating different crystal domains as identified by a bond-orientational order parameter[2]. The characteristic five-fold symmetries of Mackay icosahedra are clearly visible in the interior of all clusters (top row of Fig. 2). The larger supraparticles also showed anti-Mackay icosahedral surface terminations (bottom row of Fig. 2). Cross-sections of the internal structure are visualized in Supplementary Figs 8 and 9, and in the Supplementary Data (WebGL). Note that the assemblies made from the colloids resulted in only partially ordered clusters, where roughly half of the cluster resembled a Mackay or an anti-Mackay icosahedron, and the other half consisted of disordered colloidal particles. This was observed in all the colloidal clusters we examined, and is almost certainly due to gravitational sedimentation of the colloids within their emulsion droplets, as well as to the sedimentation and deformation of the droplets themselves.

To study the size dependence of the cluster symmetry in more detail, we examined 121 supraparticles containing between approximately 430 and 500,000 nanoparticles (with a resulting supraparticle diameter between 75 nm and 785 nm). We then determined the cluster structure from the SE-STEM images of the particles at the surface (as in Fig. 1) after having determined, for a much more limited number of supraparticles, that this was compatible with the interior structure. In the estimation of the number of nanoparticles, we assumed that the volume fraction within each supraparticle corresponded to that of hard spheres at close packing ($\Phi \approx 0.74$). As shown in Fig. 3, the transition from a Mackay icosahedron to an anti-Mackay rhombicosidodecahedron was found to be between 1,000 and 3,000 nanoparticles per supraparticle, and the transition to purely FCC ordering occurred between 25,000 and 90,000 nanoparticles. Clusters with more than 90,000 nanoparticles exhibited solely FCC ordering. We find the same three structures for micrometre-sized colloids and the core–shell semiconductor nanoparticles (Supplementary Figs 4 and 5).

The clear emergence of icosahedral symmetry in these fairly different experimental systems strongly indicates that this behaviour is not interaction specific, and poses the question of whether the formation of icosahedral clusters could be purely entropy-driven. To explore this hypothesis, we performed event-driven molecular dynamics simulations of hard spheres in a hard spherical confinement, and slowly shrunk the confining sphere, thereby mimicking the evaporation process. As shown in Fig. 2, our simulations clearly demonstrate that icosahedral ordering arises spontaneously for hard spheres in this confinement, and reveal striking agreement with the experimentally observed structures. Moreover, we studied the cluster-size dependence in simulations, and found that the transitions from Mackay to anti-Mackay to FCC ordering approximately matched those shown in Fig. 3 (Supplementary Fig. 10). In further simulations, we confirmed that the structure did not change significantly when changing the shrinking rate (corresponding to the evaporation rate) of the spherical confinement, assuming that the shrinking was sufficiently slow such that the system remained in quasi-equilibrium during the self-assembly process. Similarly, adding a short-ranged repulsion between the spheres and the confining wall, to model surface tension effects, gives rise to more faceted supraparticles, as the confinement is less severe, but does not affect the icosahedral symmetry (Supplementary Fig. 10). Furthermore, we obtained similar results in the case of an attractive wall–particle interaction (Supplementary Fig. 11).

To examine the thermodynamic stability of the icosahedral clusters, we performed free-energy calculations[31] on all the

NATURE MATERIALS DOI: 10.1038/NMAT4072

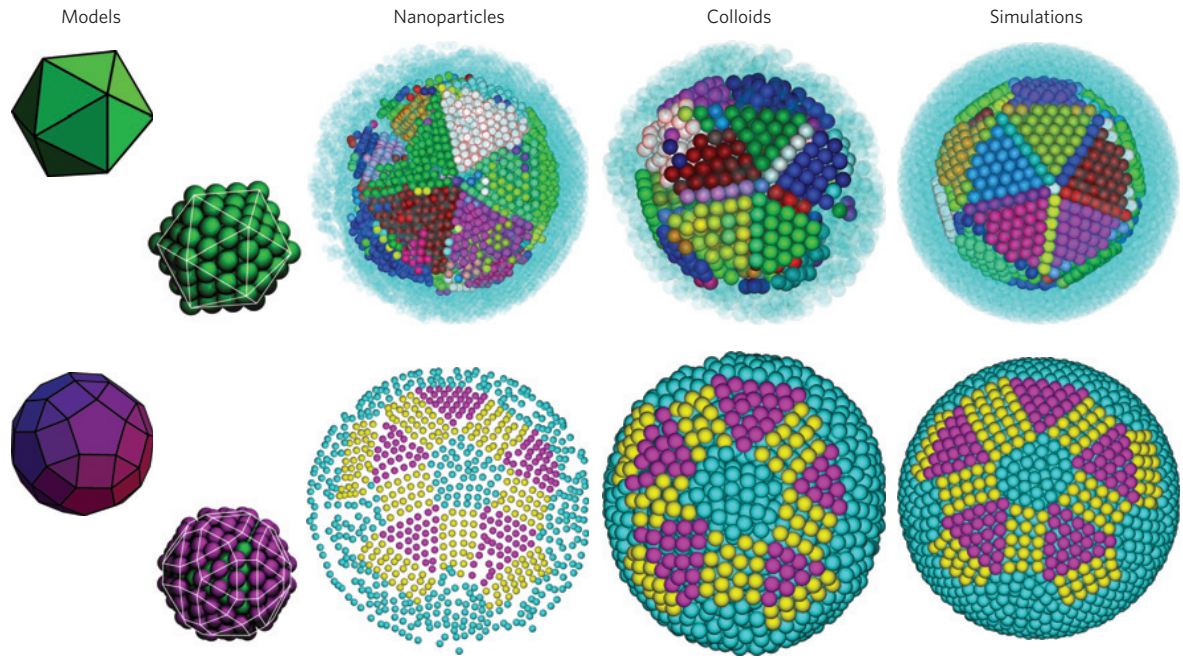

Figure 2 | Core and surface structure of the icosahedral clusters. Core (top) and surface termination (bottom) of large icosahedral supraparticles resulting from the self-assembly of spherically confined colloidal spheres. The first column depicts models of the corresponding polyhedra and their associated ideal sphere packings. The other columns contain typical examples of clusters in (from left to right) experimental systems of nanoparticles ($N \approx 12{,}000$), experimental systems of micrometre-sized colloids ($N \approx 3{,}000$), and simulations of hard spheres ($N = 6{,}000$). Note that in the top row particles belonging to the outer layers have been made transparent so that the core, which exhibits Mackay icosahedral symmetry, is readily visible. Crystalline domains are indicated by different colours. In the bottom row, the particles are coloured as a guide to the eye to highlight the anti-Mackay rhombicosidodecahedral symmetry of the clusters. See Supplementary Methods for details on particle tracking, domain identification and image processing.

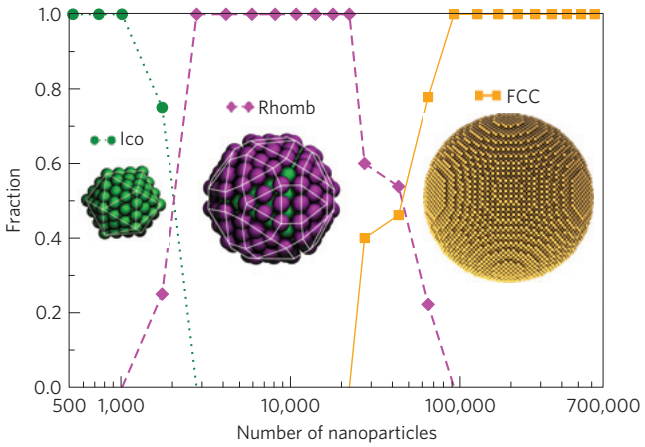

Figure 3 | Size dependence of the cluster structure. Structural transition from a Mackay icosahedron (Ico) to an anti-Mackay rhombicosidodecahedron (Rhomb) to a face-centred cubic (FCC) cluster, as observed for supraparticles consisting of nanoparticles. The fraction of structures, based on 121 supraparticles, is plotted as a function of the number of nanoparticles per supraparticle. 14 icosahedra, 63 rhombicosidodecahedra and 44 FCC clusters were observed.

structures that were observed in experiments and simulations—that is, FCC and Mackay icosahedral clusters. We compared the free energy of the two types of clusters containing between 1,500 and 4,000 particles. We found the icosahedral cluster to be more stable than the FCC for packing fractions close to melting, with free-energy differences of $0.03 \pm 0.01\ k_B T$ per particle (Supplementary Table 1). Hence, we conclude that the presence of icosahedral ordering is purely entropy-driven, and is not simply a kinetic, but rather a genuine equilibrium effect—thus explaining the high reproducibility of the icosahedral clusters. Furthermore, we remark that the free-energy differences due to entropy as reported in Supplementary Table 1 are of the same order as the potential-energy difference between icosahedral and FCC Lennard-Jones clusters[19]. Our results thus show that entropy could play an important role in determining the cluster structure even in cases where the clusters are stabilized by energetic interactions. We note here that even for small clusters the FCC structure should become stable for sufficiently high densities, as the maximum packing fraction of icosahedral clusters is $\Phi \approx 0.69$, which is significantly lower than that of a close-packed FCC cluster[6].

The evolution of the crystal structure, and thus the nucleation and growth mechanism, can also be studied directly in the simulations by identifying the crystalline particles in the system using a bond-orientational order parameter[2]. In Fig. 4 we examine the evolution of a system which forms an anti-Mackay rhombicosidodecahedron. Using the cone algorithm[10], we determine the fraction of crystalline particles in the layers near the confining wall and that of the interior as a function of packing fraction. Note that the packing fraction increases with time during the simulations, so an increase in packing fraction can also be considered as moving forward in time. We clearly see that the crystallization starts near the spherical interface, initially forming approximately two or three layers. When the packing fraction reaches approximately $\Phi = 0.52$, part of the interior starts to crystallize, growing on the already present crystalline domains in the surface layers and proceeding inwards. Furthermore, as the interior starts to crystallize, the surface layer becomes less crystalline (the decrease of the red curve in Fig. 4). Between the volume fractions $\Phi = 0.52$ and $\Phi = 0.53$, the interior completely crystallizes, forming the tetrahedral domains associated with the Mackay icosahedron. It is worth noting that this process is very

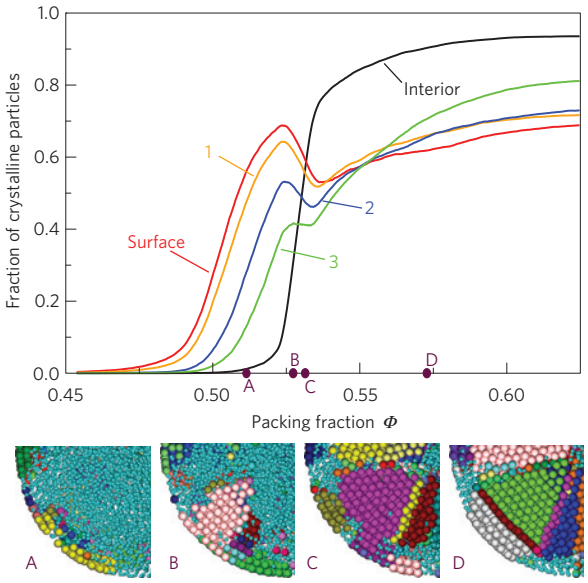

Figure 4 | Crystallization process of icosahedral clusters. Crystallization process studied by event-driven molecular dynamics simulations of 16,000 hard spheres in a shrinking spherical confinement. Top: fraction of crystalline particles in the surface layer, the first three layers and the interior as a function of the packing fraction. Note that as a result of the shrinking confinement, the packing fraction slowly increases over time. Bottom, from left to right: typical configurations from simulations at different packing fractions ($\Phi_A \approx 0.511$, $\Phi_B \approx 0.527$, $\Phi_C \approx 0.531$, $\Phi_D \approx 0.572$) as indicated on the graph. Crystalline domains are indicated with different colours. Fluid-like particles are shown with a smaller diameter and are coloured light-blue.

dynamic, as the domains can crystallize and melt several times before the system fully crystallizes into 20 tetrahedral FCC units (Supplementary Movies 3 and 4). On further increasing the packing fraction, the surface layers recrystallize into the anti-Mackay surface termination. This crystallization process is reminiscent of the nucleation of hard spheres near hard spherical seeds[32]. In this case, crystal nucleation starts on the surface of the seed, which then grows out into the bulk, whereas the crystal near the surface melts. In contrast, our simulations of smaller numbers of confined hard spheres, which self-assemble into Mackay icosahedra, did not exhibit melting or recrystallization (Supplementary Fig. 12).

In conclusion, we showed that entropy and spherical confinement alone are sufficient for the formation of stable icosahedral clusters. Our simulations clearly demonstrate that energetic interactions between the particles are not required for icosahedral order. Interestingly, this also provides new insights regarding the results reported in ref. 11: whereas the authors of that study attributed the formation of icosahedral clusters of gold nanoparticles to energetic interactions, it is now clear that entropic contributions should not be overlooked. Furthermore, as already argued in ref. 11, we clearly find that the interaction between the particles and the interface does not seem to play an important role in this self-assembly process. In fact, our simulations show similar results regardless of whether the interface–particle interaction is attractive, hard, or repulsive. Our results also provide an interesting contrast to the icosahedral order observed in much smaller ($N = 12$) clusters of particles[33]. In such systems, it was argued that the structure of the clusters was mainly determined by capillary forces during the final stages of the evaporation process, resulting in clusters that minimized the second moment of the mass distribution[34]. Here, we find that the spherical confinement provided by the surface tension of emulsion droplets is sufficient for the formation of large icosahedral clusters that minimize the free energy. As a consequence, we speculate that our results obtained with emulsions will probably be similar to those obtained in the more general case of the slow drying of droplets of colloidal dispersions. It remains for future work to analyse to what extent the entropy contributes in stabilizing clusters of particles with long-ranged attractions, if it is possible to increase the size range of equilibrium icosahedral supraparticles using particles with long-range interactions, and how the present results can be extended to (hard) binary systems.

The fact that spherical confinement can stabilize structures that are fully incommensurate with that of the bulk, suggests new ways of designing small crystals with unusual symmetries that may be beneficial for optical or other applications. This opens up a new avenue for the self-assembly of novel structures by combining the vast array of colloidal building blocks available at present (for example, rods, dumbbells), and mixtures thereof. Furthermore, the resulting supraparticles themselves can in turn self-assemble[35], resulting in hierarchical structures with new functionalities added at different length scales—for example, with plasmonic properties at the nanoscale and photonic properties at the micrometre scale.

Methods

Experiments. For the nanoparticle supraparticles, 6.0 nm (9 nm effective, including the oleic acid ligands) cobalt iron oxide nanoparticles[26] were dispersed in cyclohexane and mixed with water containing sodium dodecyl sulfate and dextran. The mixture was sheared at a shear rate of 1.56×10^{-5} s^{-1} and the resulting oil-in-water emulsion was heated at 68 °C for four hours. The resulting supraparticles were washed by centrifugation and freeze-dried on a carbon-coated TEM grid. The supraparticles were analysed using electron tomography[29]. For the colloidal supraparticles, 1.32 μm fluorescent core–shell silica colloids[27] were dispersed in de-ionized water. The suspension was added to hexadecane containing the surfactant Span 80 and shaken. The resulting water-in-oil emulsion was left to evaporate, and the obtained supraparticles were analysed using quantitative 3D confocal microscopy[30]. To identify the crystalline domains, a cluster criterion based on local bond-order parameters[2] was used. For a detailed description of the chemicals and equipment used, see the Supplementary Methods.

Simulations. We perform event-driven molecular dynamics (EDMD) simulations of hard spheres with a diameter σ confined in a spherical cavity. To model the spherical confinement, we use three types of external potential that act on the hard spheres: an impenetrable hard spherical wall of radius R, a soft repulsive wall–particle potential with an interaction range $\leq 2\sigma$, and an attractive wall–particle potential with an interaction range of σ. To mimic the solvent evaporation of the emulsion droplets, the radius of the spherical cavity is slowly reduced at a constant compression speed $v \leq 10^{-4}\sigma/\tau$, where $\tau = \sqrt{m\sigma^2/k_B T}$ is the EDMD time unit, m the mass of a particle, k_B the Boltzmann constant and T the temperature. We use an Andersen thermostat to keep the temperature of the system constant during the simulations. To identify the crystalline particles, we used the same procedure as for the experimental data. In addition, we employed the cone algorithm[10] to study the crystallization mechanism.

We calculate the free energy of both FCC clusters and icosahedral clusters using a three-step thermodynamic integration method proposed in ref. 31. In particular, this method allows us to calculate the free-energy difference between our system—for example, spherically confined hard spheres—and a reference system for which the free energy is known exactly. The reference system we use consists of non-interacting particles attached, via a linear well potential, to lattice sites. The lattice sites are taken from representative configurations of the system featuring the desired cluster symmetry. In the first integration step, the coupling between the particles and their respective lattice sites is slowly turned on. To accurately perform this integration, we sampled more than 300 values of the coupling constant, and fit the results with an Akima spline before performing the integration. The other two integration steps consist of slowly switching off the hard interactions in the model—namely, the particle–particle and particle–wall interactions. These last two integrations were done using a standard 20-point Gauss–Legendre integration scheme.

More simulation details are reported in the Supplementary Methods.

Received 24 April 2014; accepted 30 July 2014; published online 31 August 2014

References

1. Nelson, D. R. & Halperin, B. I. Pentagonal and icosahedral order in rapidly cooled metals. *Science* **229,** 233–238 (1985).
2. Steinhardt, P. J., Nelson, D. R. & Ronchetti, M. Bond-orientational order in liquids and glasses. *Phys. Rev. B* **28,** 784–805 (1983).
3. Doye, J. P. K. & Wales, D. J. The structure and stability of atomic liquids: From clusters to bulk. *Science* **271,** 484–487 (1996).
4. Karayiannis, N. C., Malshe, R., Kröger, M., de Pablo, J. J. & Laso, M. Evolution of fivefold local symmetry during crystal nucleation and growth in dense hard-sphere packings. *Soft Matter* **8,** 844–858 (2012).
5. Bernal, J. D. & Finney, J. L. Random close-packed hard-sphere model. II. Geometry of random packing of hard spheres. *Discuss. Faraday Soc.* **43,** 62–69 (1967).
6. Mackay, A. L. A dense non-crystallographic packing of equal spheres. *Acta Crystallogr.* **15,** 916–918 (1962).
7. Doye, J. P. K. & Wales, D. J. Thermally-induced surface reconstructions of Mackay icosahedra. *Z. Phys. D* **40,** 466–468 (1997).
8. Meng, G., Arkus, N., Brenner, M. P. & Manoharan, V. N. The free-energy landscape of clusters of attractive hard spheres. *Science* **327,** 560–563 (2010).
9. Hendy, S. C. & Doye, J. P. K. Surface-reconstructed icosahedral structures for lead clusters. *Phys. Rev. B* **66,** 235402 (2002).
10. Wang, Y., Teitel, S. & Dellago, C. Melting of icosahedral gold nanoclusters from molecular dynamics simulations. *J. Chem. Phys.* **122,** 214722 (2005).
11. Lacava, J., Born, P. & Kraus, T. Nanoparticle clusters with Lennard-Jones geometries. *Nano Lett.* **12,** 3279–3282 (2012).
12. Frank, F. C. Supercooling of liquids. *Proc. R. Soc. Lond. A* **215,** 43–46 (1952).
13. Pusey, P. N. & Van Megen, W. Phase behaviour of concentrated suspensions of nearly hard colloidal spheres. *Nature* **320,** 340–342 (1986).
14. Bolhuis, P. G., Frenkel, D., Mau, S-C. & Huse, D. A. Entropy difference between crystal phases. *Nature* **388,** 235–236 (1997).
15. Conway, J. H. & Sloane, N. J. A. *Sphere Packings, Lattices and Groups* (Springer, 1998).
16. McGinley, J. T., Jenkins, I., Sinno, T. & Crocker, J. C. Assembling colloidal clusters using crystalline templates and reprogrammable DNA interactions. *Soft Matter* **9,** 9119–9128 (2013).
17. O'Malley, B. & Snook, I. Crystal nucleation in the hard sphere system. *Phys. Rev. Lett.* **90,** 085702 (2003).
18. Hubert, H. *et al.* Icosahedral packing of B_{12} icosahedra in boron suboxide (B_6O). *Nature* **391,** 376–378 (1998).
19. Doye, J. P. K. & Calvo, F. Entropic effects on the structure of Lennard-Jones clusters. *J. Chem. Phys.* **116,** 8307–8317 (2002).
20. Hofmeister, H. Forty years study of fivefold twinned structures in small particles and thin films. *Cryst. Res. Technol.* **33,** 3–25 (1998).
21. Langille, M. R., Zhang, J., Personick, M. L., Li, S. & Mirkin, C. A. Stepwise evolution of spherical seeds into 20-fold twinned icosahedra. *Science* **337,** 954–957 (2012).
22. Tang, J. *et al.* Hard-sphere packing and icosahedral assembly in the formation of mesoporous materials. *J. Am. Chem. Soc.* **129,** 9044–9048 (2007).
23. Wales, D. J. Surveying a complex potential energy landscape: Overcoming broken ergodicity using basin-sampling. *Chem. Phys. Lett.* **584,** 1–9 (2013).
24. Fortini, A. & Dijkstra, M. Phase behaviour of hard spheres confined between parallel hard plates: Manipulation of colloidal crystal structures by confinement. *J. Phys. Condens. Matter* **18,** L371–L378 (2006).
25. Löwen, H., Oguz, E. C., Assoud, L. & Messina, R. Colloidal crystallization between two and three dimensions. *Adv. Chem. Phys.* **148,** 225–249 (2012).
26. Bodnarchuk, M. I. *et al.* Exchange-coupled bimagnetic wüstite/metal ferrite core/shell nanocrystals: Size, shape, and compositional control. *Small* **5,** 2247–2252 (2009).
27. Van Blaaderen, A. & Vrij, A. Synthesis and characterization of colloidal dispersions of fluorescent, monodisperse silica spheres. *Langmuir* **8,** 2921–2931 (1992).
28. Farges, J., De Feraudy, M. F., Raoult, B. & Torchet, G. Noncrystalline structure of argon clusters. II. Multilayer icosahedral structure of Ar_N clusters $50 < N < 750$. *J. Chem. Phys.* **84,** 3491–3501 (1986).
29. Friedrich, H. *et al.* Quantitative structural analysis of binary nanocrystal superlattices by electron tomography. *Nano Lett.* **9,** 2719–2724 (2009).
30. Van Blaaderen, A. & Wiltzius, P. Real-space structure of colloidal hard-sphere glasses. *Science* **270,** 1177–1179 (1995).
31. Schilling, T. & Schmid, F. Computing absolute free energies of disordered structures by molecular simulation. *J. Chem. Phys.* **131,** 231102 (2009).
32. Cacciuto, A., Auer, S. & Frenkel, D. Onset of heterogeneous crystal nucleation in colloidal suspensions. *Nature* **428,** 404–406 (2004).
33. Manoharan, V. N., Elsesser, M. T. & Pine, D. J. Dense packing and symmetry in small clusters of microspheres. *Science* **301,** 483–487 (2003).
34. Lauga, E. & Brenner, M. P. Evaporation-driven assembly of colloidal particles. *Phys. Rev. Lett.* **93,** 238301 (2004).
35. Bai, F. *et al.* A versatile bottom-up assembly approach to colloidal spheres from nanocrystals. *Angew. Chem. Int. Ed.* **46,** 6650–6653 (2007).

Acknowledgements

We thank R. J. A. Moes (who is funded by the FOM programme Control over Functional Nanoparticle Solids (FNPS)) for synthesis of the semiconductor particles, A. Kuijk for the synthesis of the silica colloids, and T. H. Besseling for the two-dimensional tracking. We thank J. R. Edison, W. Vlug and R. v. Roij for critical reading of the manuscript. B.d.N. acknowledges financial support from a 'Nederlandse Organisatie voor Wetenschappelijk Onderzoek' (NWO) CW grant. M.D. and F.S. acknowledge financial support from an NWO-VICI grant. S.D. and M.D. acknowledge financial support from an NWO-CW-Echo grant.

Author contributions

A.I. and A.v.B. initiated the experimental part of the project. B.d.N. and D.J.G. performed the experiments under the supervision of A.I. and A.v.B. B.d.N. and J.D.M. performed the electron microscopy analysis. S.D. and F.S. carried out the simulations under the supervision of L.F. and M.D. B.d.N., S.D., F.S., L.F., M.D. and A.v.B. co-wrote the paper. All authors analysed and discussed results.

Additional information

Supplementary information is available in the online version of the paper. Reprints and permissions information is available online at www.nature.com/reprints. Correspondence and requests for materials should be addressed to A.v.B. or M.D.

Competing financial interests

The authors declare no competing financial interests.